Areas of High ^{18}F-FDG Uptake on Preradiotherapy PET/CT Identify Preferential Sites of Local Relapse After Chemoradiotherapy for Non–Small Cell Lung Cancer

Jérémie Calais[1,2], Sébastien Thureau[1–3], Bernard Dubray[2,3], Romain Modzelewski[1–3], Luc Thiberville[2,4], Isabelle Gardin[1–3], and Pierre Vera[1,2]

[1]Nuclear Medicine Department, Henri Becquerel Cancer Center and Rouen University Hospital, Rouen, France; [2]QuantIF–LITIS (EA [Equipe d'Accueil] 4108–FR CNRS [Fédération de Recherche–Centre National pour la Recherche Scientifique] 3638), Faculty of Medicine, University of Rouen, Rouen, France; [3]Department of Radiotherapy and Medical Physics, Henri Becquerel Cancer Centre and Rouen University Hospital, Rouen, France; and [4]Department of Pneumology, Rouen University Hospital, Rouen, France

The high rates of failure in the radiotherapy target volume suggest that patients with stage II or III non–small cell lung cancer (NSCLC) should receive an increased total dose of radiotherapy. Areas of high ^{18}F-FDG uptake on preradiotherapy ^{18}F-FDG PET/CT have been reported to identify intratumor subvolumes at high risk of relapse after radiotherapy. We wanted to confirm these observations on a cohort of patients included in 3 sequential prospective studies. Our aim was to assess an appropriate threshold (percentage of maximum standardized uptake value [SUV_{max}]) to delineate subvolumes on staging ^{18}F-FDG PET/CT scans assuming that a smaller target volume would facilitate isotoxic radiotherapy dose escalation. **Methods:** Thirty-nine patients with inoperable stage II or III NSCLC, treated with chemoradiation or with radiotherapy alone, were extracted from 3 prospective studies (ClinicalTrials.gov identifiers NCT01261585, NCT01261598, and RECF0645). All patients underwent ^{18}F-FDG PET/CT at initial staging, before radiotherapy, during radiotherapy, and during systematic follow-up in a single institution. All ^{18}F-FDG PET/CT acquisitions were coregistered on the initial scan. Various subvolumes in the initial acquisition (30%, 40%, 50%, 60%, 70%, 80%, and 90% SUV_{max} thresholds) and in the 3 subsequent acquisitions (40% and 90% SUV_{max} thresholds) were pasted on the initial scan and compared. **Results:** Seventeen patients had a local relapse. The SUV_{max} measured during radiotherapy was significantly higher in locally relapsed tumors than in locally controlled tumors (mean, 6.8 vs. 4.6; $P = 0.02$). The subvolumes delineated on initial PET/CT scans with 70%–90% SUV_{max} thresholds were in good agreement with the recurrent volume at a 40% SUV_{max} threshold (common volume/baseline volume, 0.60–0.80). The subvolumes delineated on initial PET/CT scans with 30%–60% SUV_{max} thresholds were in good to excellent agreement with the core volume of the relapse (90% SUV_{max} threshold) (common volume/recurrent volume and overlap fraction indices, 0.60–0.93). The agreement was moderate (>0.51) when a 70% SUV_{max} threshold was used to delineate on initial PET/CT scans. **Conclusion:** High ^{18}F-FDG uptake areas on pretreatment PET/CT scans identify tumor subvolumes at greater risk of relapse in patients with NSCLC treated by concomitant chemoradiation. We propose a 70% SUV_{max} threshold to delineate areas of high ^{18}F-FDG uptake on initial PET/CT scans as the target volumes for potential radiotherapy dose escalation.

Key Words: ^{18}F-FDG PET/CT; lung cancer; radiotherapy; target volume; ^{18}F-FDG uptake; local relapse

J Nucl Med 2015; 56:196–203
DOI: 10.2967/jnumed.114.144253

The survival probability of patients with stage II or III non–small cell lung cancer (NSCLC) remains low after curative-intent chemoradiotherapy (*1,2*). Many relapses occur within the radiotherapy target volume, thereby suggesting an insufficient total dose of radiotherapy (*3–5*). Therefore, reduction of the target volume is expected to allow isotoxic dose escalation (*6*). Such an approach would benefit from recent improvements in stereotactic body radiotherapy with imaging-guided radiotherapy and intensity-modulated radiotherapy to improve the precision of radiotherapy delivery (*6,7*). A possible way to achieve this goal would be to take advantage of intratumor heterogeneity by specific targeting of treatment-resistant tumor subvolumes. The tumor subvolumes with high ^{18}F-FDG uptake (standardized uptake value [SUV] > 50% of the maximum SUV [SUV_{max}]) on preradiotherapy PET/CT have been reported to identify intratumor subvolumes that have a high risk of relapse after radiotherapy (*8–11*). The delivery of higher radiotherapy doses to these reduced target volumes was investigated in a randomized phase II study and seemed feasible (*12*). Our group has conducted 3 prospective studies (*13–15*) addressing the feasibility and role of ^{18}F-FDG PET/CT during curative-intent chemoradiotherapy in 67 NSCLC patients. We selected 39 patients with a complete set of ^{18}F-FDG PET/CT data who were analyzed in our institution (CHB, Rouen). Our aim was to investigate whether a higher (>50%) SUV_{max} threshold on initial ^{18}F-FDG PET/CT scans would still define tumor subvolumes at high risk for relapse, assuming that a smaller volume would facilitate radiotherapy dose escalation.

MATERIALS AND METHODS

Patient Population

Data were extracted from 3 prospective studies (RTEP1, RTEP2, and RTEP4) registered on ClinicalTrials.gov (identifiers NCT01261585, NCT01261598, and RECF0645, respectively) and approved by the institutional review board for human studies (*13–15*). Sixty-seven patients

Received Jun. 10, 2014; revision accepted Dec. 8, 2014.
For correspondence or reprints contact: Pierre Vera, Department of Nuclear Medicine, Centre Henri Becquerel, Rue d'Amiens, 76000 Rouen, France.
E-mail: pierre.vera@chb.unicancer.fr
Published online Jan. 8, 2015.

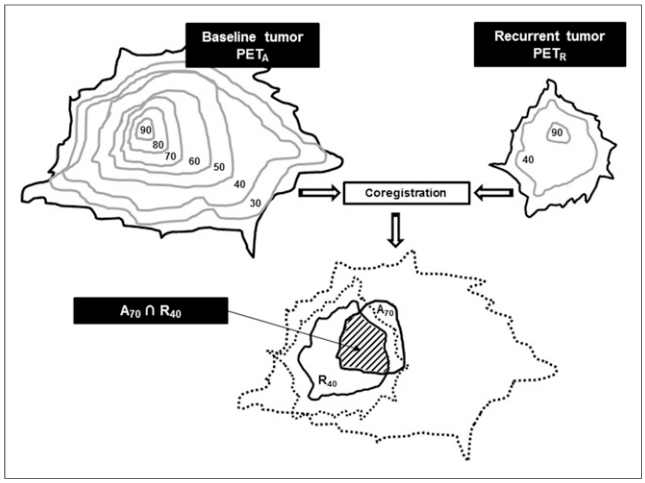

FIGURE 1. Estimation of typical overlapping of A_{70} and R_{40} subvolumes after coregistration and reports. Numbers indicate SUV_{max} thresholds as percentages.

with inoperable stage II or III NSCLC had been treated with chemoradiotherapy or with radiotherapy alone. The included patients were those who underwent ^{18}F-FDG PET/CT at initial staging, before radiotherapy, during radiotherapy (42 Gy), and during systematic follow-up (3 mo and 1 y) in a single center (CHB, Rouen). Thirty-nine patients with complete clinical and imaging data available were selected for the present study. All patients gave written informed consent before inclusion.

^{18}F-FDG PET/CT Imaging

The ^{18}F-FDG PET/CT data were acquired on a Biograph Sensation 16 Hi-Rez device (Siemens Medical Solutions). The patients were required to fast for at least 6 h before imaging to ensure that the serum glucose and endogenous serum insulin levels were low at the time of ^{18}F-FDG administration. A 5 MBq/kg dose of ^{18}F-FDG was injected after 20 min of rest. Sixty minutes later ($\pm$10 min), the acquisition began with noninjected CT in the cephalocaudad direction. The images were acquired with the patients' arms positioned over the head while they were breathing freely. The PET data were then acquired in the caudocephalad direction using a whole-body protocol (3 min per bed position). The acquisition time was adapted as a function of the injected activity (regarding the standard 5 MBq/kg) and the delay between the injection and acquisition (standardized to 60 min) to obtain a normalized counting rate for all patients. Six to 8 bed positions per patient were acquired, and the axial field of view for 1 bed position was 162 mm with a bed overlap of 25% (plane spacing, 2 mm). The PET images were reconstructed using Fourier rebinning and attenuation-weighted ordered-subset expectation maximization with clinical software. The images were corrected for random coincidences, scatter, and attenuation using the CT scan data. The ^{18}F-FDG PET images were smoothed with a gaussian filter (full width at half maximum, 5 mm).

For each patient, the first ^{18}F-FDG PET/CT scan (PET_A) was obtained at initial staging, followed by a second ^{18}F-FDG PET/CT scan before radiotherapy if induction chemotherapy was administered (PET_B). A third ^{18}F-FDG PET/CT scan (PET_C) was obtained during the fifth week of radiotherapy, at an approximate dose of 40–45 Gy. A fourth ^{18}F-FDG PET/CT scan was acquired during systematic follow-up (3 mo and 1 y) or if there was a suspected relapse (PET_R).

^{18}F-FDG PET/CT Analysis

The 156 PET/CT scans acquired for the 39 selected patients were analyzed in consensus by two senior physicians (a nuclear medicine specialist and a radiation oncology specialist) in a single center (Henri Becquerel Center, Rouen) on a Planet Onco workstation (Planet Onco, version 2.0; DOSISoft).

The SUV_{max} and metabolic tumor volume data were collected. The metabolic tumor volume was defined with a threshold at 40% of tumor SUV_{max} since this value is widely used to delineate volumes with significant ^{18}F-FDG uptake (*16,17*). For each patient, all PET/CT acquisitions were coregistered on the initial CT scan, focusing on the tumor, with a rigid registration method (block-matching rigid registration method (*18*)). The physicians were allowed to manually adjust the registration to avoid obvious misregistration (pleural effusion, pulmonary retraction, radiation-induced pneumonitis, tumor volume decrease, respiration motion, or change in patient position). The PET_A scan was systematically used as a reference. In total, 117 coregistrations were performed.

We defined 507 volumes of interest: 7 on PET_A and 2 each on PET_B, PET_C, and PET_R. On PET_A, the baseline subvolumes were delineated using a relative threshold method (30%, 40%, 50%, 60%, 70%, 80%, and 90% of primary tumor SUV_{max}, with the corresponding volumes being referred to as A_{30}, A_{40}, A_{50}, A_{60}, A_{70}, A_{80}, and A_{90}, respectively). On PET_B, 40% and 90% of SUV_{max} were used as thresholds to delineate the B_{40} and B_{90} subvolumes, respectively. The same process was applied to PET_C (C_{40} and C_{90}) and PET_R (R_{40} and R_{90}). Each subvolume of PET_A was then reported on PET_B, PET_C, and PET_R, and each subvolume of PET_B, PET_C, and PET_R was reported on PET_A, to quantify their respective overlaps as shown in Figure 1.

Overlap Quantification

Our objective was to find the highest threshold (as a percentage of SUV_{max}) delineating the smallest subvolume on baseline PET yielding the highest overlap index compared with the relapse volume (PET_R) and compared with the metabolically active residual-disease volumes during the therapeutic sequence (PET_B and PET_C).We investigated all potential overlaps between the above-defined volumes of interest: baseline tumor (A_{30}–A_{90}) versus postinduction chemotherapy tumor subvolumes (B_{40} and B_{90}), per-radiotherapy subvolumes (C_{40} and C_{90}), and relapse subvolumes (R_{40} and R_{90}). The following 5 indices were used: the Dice index ($2 \times \frac{V_1 \cap V_2}{V_1 + V_2}$), the Jaccard index ($\frac{V_1 \cap V_2}{V_1 \cup V_2}$), the overlap fraction ($\frac{V_1 \cap V_2}{\min(V_1, V_2)}$), the common volume divided by the initial volume ($\frac{V_1 \cap V_2}{V_1}$), and the common volume divided by the compared volume ($\frac{V_1 \cap V_2}{V_2}$).

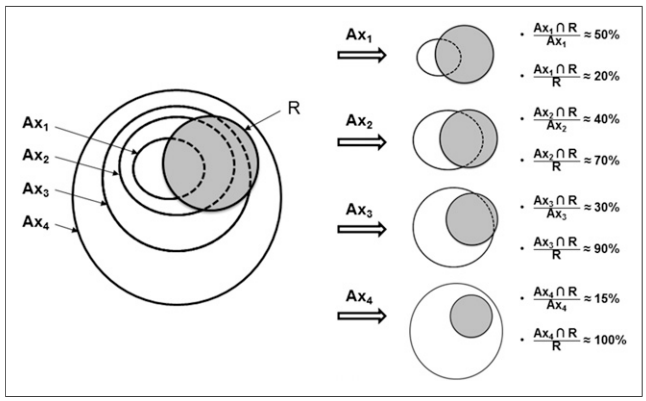

FIGURE 2. Study flow for scenario of PET_A and PET_R subvolume comparisons. Shown are indices of common volume (A∩R), with A referring to staging ^{18}F-FDG PET/CT and R to ^{18}F-FDG PET/CT at recurrence.

TABLE 1
Patient Demographics and Characteristics

Characteristic	Details	Total	CR	LR	DR
Mean age (y)		58 (39–77)	59 (39–77)	58 (46–74)	59 (40–76)
Sex	Male	31 (79)	7 (64)	15 (88)	9 (81)
	Female	8 (21)	4 (36)	2 (12)	2 (18)
Histology	SCC	21 (54)	2 (18)	14 (82)	5 (45)
	ADC	10 (26)	5 (45)	1 (6)	4 (36)
	LCUC	8 (20)	4 (36)	2 (12)	2 (18)
TNM stage	IIa	3 (8)	1 (9)	11 (6)	1 (9)
	IIb	2 (5)	1 (9)	1 (6)	0
	IIIa	15 (38)	4 (36)	8 (47)	3 (27)
	IIIb	19 (49)	5 (45)	7 (41)	7 (64)
Location of tumor	RSL	19 (39)	5 (45)	6 (35)	8 (73)
	RML	3 (8)	1 (9)	2 (12)	0
	RIL	3 (8)	2 (18)	1 (6)	0
	LSL	11 (28)	3 (27)	6 (35)	2 (18)
	LIL	4 (10)	0	3 (18)	1 (9)
Induction chemotherapy	Yes	33 (85)	9 (81)	13 (76)	10 (91)
	No	6 (15)	2 (18)	4 (24)	1 (9)
Dose (Gy)	At PET_C	44 (40–52)	45 (42–50)	45 (40–52)	43 (40–46)
	Total	67 (60–70)	66 (60–70)	67 (60–70)	68 (66–70)
Time of follow-up (mo)		30 (6–76)	46 (18–76)	22 (6–60)	27 (11–51)
RT duration (d)		48 (39–66)	47 (41–53)	48 (39–66)	48 (45–52)
SUV_{max}	PET_A	11.0 (3.7–22.1)	11.7 (5.5–18.1)	11.7 (3.7–22.1)	10.9 (5.1–16.6)
	PET_B	8.4 (1.2–20.8)	7.5 (1.2–15.2)	9.1 (2.5–18.9)	8.4 (2.8–20.8)
	PET_C	5.6 (0.8–13.1)	4 (0.8–5.9)	6.8 (2.3–11.9)	5.2 (1.1–3.15)
MTV (cm^3)	PET_A (A_{40})	54.0 (2.4–176.3)	44.8 (6.6–125.8)	63.8 (10.6–176.3)	47.0 (2.4–103.2)
	PET_B (B_{40})	26.2 (1.7–86.6)	18.2 (0.7–31.2)	32.4 (9.2–86.6)	24.8 (1.5–73.4)
	PET_C (C_{40})	30.9 (0.8–77.8)	28.6 (0.8–77.6)	34 (4.2–76.2)	5.2 (2.9–57.8)

SCC = squamous cell carcinoma; ADC = adenocarcinoma; LCUC = large cell undifferentiated carcinoma; RSL = right superior lobe; RML = right median lobe; RIL = right inferior lobe; LSL = left superior lobe; LIL: = left inferior lobe; RT = radiotherapy; MTV = metabolic tumor volume.

Data in parentheses are percentages or ranges.

The Dice, Jaccard, and overlap fraction indices are widely used to compare delineated volumes obtained with different methods or by multiple investigators (*19*). Their values vary between 0 (if the volumes are completely disjointed) and 1 (if the volumes match perfectly in size, shape, and location). They can be misleading when the sizes of the delineated volumes differ. The $A_x \cap R_{40}/A_x$ was used to estimate the larger subvolume with high chances of containing the recurrent tumor volume (R_{40}), aiming to limit the irradiation of areas with a low risk of recurrence.

TABLE 2
Subvolumes Delineated with Various SUV_{max} Thresholds

Stage	Volume 30 (cm^3)	Volume 40 (cm^3)	Volume 50 (cm^3)	Volume 60 (cm^3)	Volume 70 (cm^3)	Volume 80 (cm^3)	Volume 90 (cm^3)	SUV_{max}
A	76.2 (60.4)	53.7 (45.6)	37.0 (33.7)	22.6 (21.6)	11.8 (11.8)	4.5 (5.5)	0.92 (1.3)	11.4 (4.4)
B		26.2 (21.6)					0.45 (0.45)	8.4 (4.2)
C		30.9 (21.9)					0.44 (0.79)	5.6 (2.8)
R		60.0 (65.1)					0.50 (0.4)	6.0 (2.6)

Numeric indices refer to threshold for delineation. Data are mean followed by SD within parentheses.

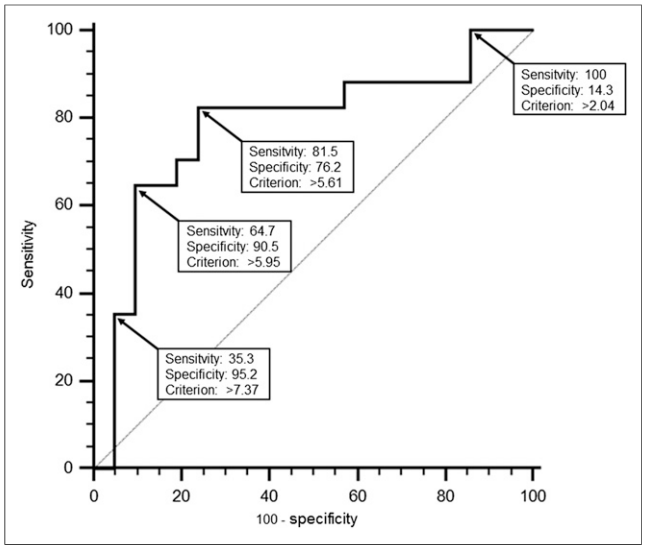

FIGURE 3. Receiver-operating-characteristic curve analysis of SUV_{max} as predictor of LR.

The $A_x \cap R_{90}/R_{90}$ index was used to estimate the smaller subvolume on PET_A containing the highest uptake area in the recurrent tumor (R_{90}), to avoid omitting areas at high risk of recurrence from the target volume.

A schematic example of the interpretation of overlap indices is shown in Figure 2.

Statistics

To classify the quality of overlap, we chose the criteria used for the Cohen κ test when assessing the agreement between investigators: 0–0.2, poor agreement; 0.21–0.40, fair agreement; 0.41–0.60, moderate agreement; 0.61–0.80, good agreement; and 0.81–1.00, very good agreement (*15*).

The mean and SD were used for descriptive statistics. The association between ^{18}F-FDG PET/CT and clinical parameters was tested using repeated-measures ANOVA and the χ^2 test. A P value of less than 0.05 was considered statistically significant (bilateral test). All analyses were performed using MedCalc Statistical Software, version 12.7.2 (MedCalc Software bvba).

RESULTS

Patient Characteristics

Of the 67 patients included in the RTEP studies, 39 (RTEP1, 9/10; RTEP2, 23/52; RTEP4, 4/5) were eligible for the present study (Table 1). The noneligible patients were those for whom the full set of sequential ^{18}F-FDG PET/CT scans was not available (patients who were treated in another center or scans with technical problems).

The mean follow-up of the total studied population was 30 ± 19 mo. Eleven patients remained in complete metabolic response (CR). Seventeen patients had a local relapse (LR) with or without nodal or metastatic disease. We considered metabolically persistent residual disease and local recurrence to be equal. Eleven patients had a distant dissemination (nodal or metastatic) without local residual disease (DR). Ipsilateral (outside the initial radiotherapy target volume) or contralateral lung recurrence was considered metastasis. Metastasis occurred in 16 patients.

A manual adjustment of the coregistered images was required in 10 patients. No significant differences were observed when the overlap indices were compared with those obtained in 7 patients without manual adjustment. All patients were pooled for further analyses. The volume measurements in LR patients are summarized in Table 2. The mean initial tumor metabolic volume (A_{40}) was 54 cm^3 (range, 2.4–176 cm^3; SD, 46 cm^3), and the mean A_{70} subvolume was 12 cm^3 (range, 0.6–51 cm^3; SD, 12 cm^3).

Univariate Analysis

When LR (n = 17), DR (n = 11), and CR (n = 11) patients were compared, there were no significant differences in age; sex; TNM stage; tumor location; induction chemotherapy; radiotherapy dose and duration; tumor metabolic volume at PET_A, at PET_B, and PET_C (threshold = 40% SUV_{max}); or SUV_{max} at PET_A and PET_B. None of these parameters was significantly different in the 16 metastatic patients.

The frequency of LR was higher for squamous cell carcinoma (14/21, 66%) than for adenocarcinoma (1/10, 10%) or undifferentiated carcinoma (2/8, 25%) (P = 0.03).

The SUV_{max} measured on PET_C was significantly higher in relapsing tumors than in locally controlled tumors (mean, 6.8 vs. 4.6; P = 0.02). The area under the receiver-operating-characteristic curve was 0.78 (95% confidence interval, 0.62–0.90) (Fig. 3). An SUV_{max} of more than 5.6 (i.e., the mean of SUV_{max} observed in the locally relapsed and controlled groups) yielded a sensitivity of 82% (95% confidence interval, 57%–96%) and a specificity of 76% (95% confidence interval, 53%–92%) to predict LR.

Overlap Comparisons

We obtained 6,650 indices corresponding to 1,330 potential overlaps of 507 volumes of interest on the 156 PET/CT scans. Overlap comparisons of PET_A subvolumes with PET_B and PET_C subvolumes were performed for all 39 included patients. Overlap comparisons between PET_A and PET_R subvolumes were performed only for the 17 LR patients. An example is shown in Figure 4. The mean overlap indices are reported in Figure 5 (Details are provided in Supplemental Fig. 1; supplemental materials are available at http://jnm.snmjournals.org).

A_x Versus B_{40}, C_{40}, and R_{40} Comparisons

We first tried to identify an SUV_{max} threshold on PET_A scans that would consistently delineate a volume that included the areas with significant ^{18}F-FDG uptake (40% SUV_{max}) on subsequent PET scans (panels A, C, and E in Fig. 5).

The overlap fractions between the PET_A scans and the PET_B, PET_C, and PET_R scans showed good agreement (between 0.60 and 0.80) for all initial SUV_{max} thresholds (except $A_{80} \cap C_{40}$ and $A_{90} \cap C_{40}$, which were slightly below 0.60). The $A_x \cap R_{40}/A_x$ indices between PET_A scans and PET_R scans at the time of recurrence showed good agreement (values between 0.60 and 0.80) for A_x SUV_{max} thresholds between 70% and 90%. The $A_x \cap R_{40}/R_{40}$ index was good only for the 30% SUV_{max} threshold. The Dice and Jaccard indices showed poor to moderate agreement. The low variations between panels A, C, and E indicate that the position of the subvolumes was similar during the therapeutic sequence.

A_x Versus B_{90}, C_{90}, and R_{90} Comparisons

We then investigated whether the areas with high ^{18}F-FDG uptake (with a 90% SUV_{max} threshold) on subsequent PET scans could be identified on the PET_A scans (panels B, D, and F in Fig. 5).

Good to excellent overlap fractions (0.60–0.93) were obtained for the volumes delineated on PET_A with SUV_{max} thresholds between 30% and 60%. Similarly, high values for the $A_x \cap R_{90}/R_{90}$

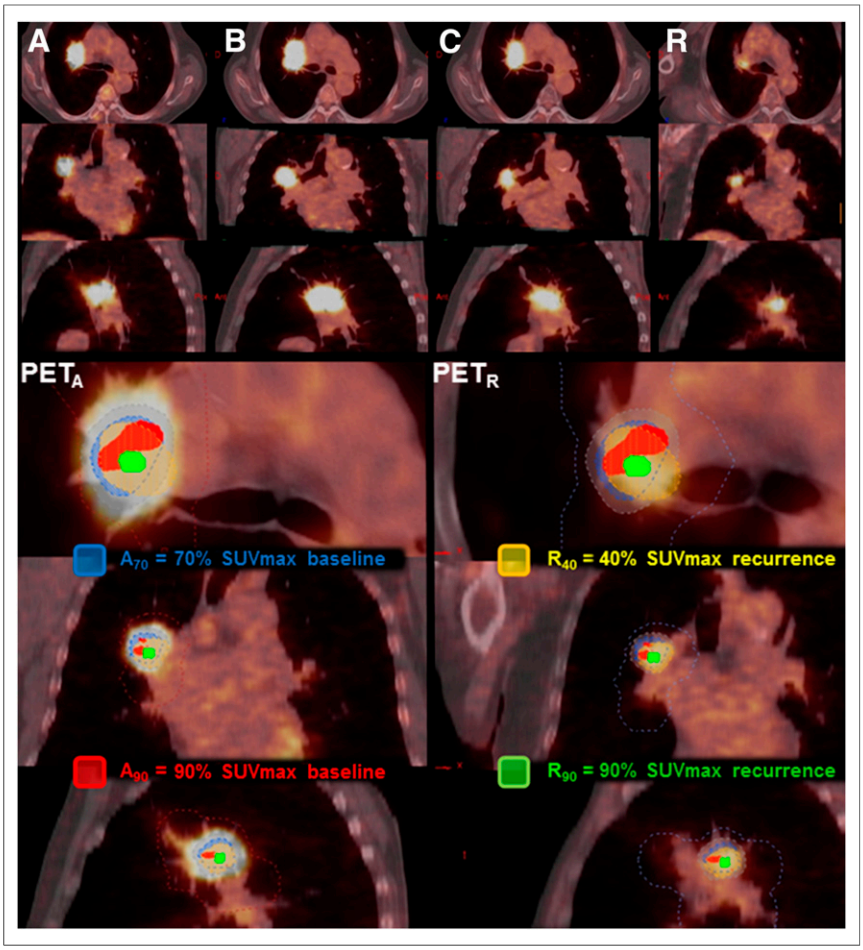

FIGURE 4. Example of 74-y-old man with right superior lobe squamous cell carcinoma T3N0M0. Shown are staging PET_A (A), PET_B (B), PET_C (C), and PET_R (R). Numeric indices refer to threshold for delineation. A_{70} and A_{90} subvolumes were reported on PET_R, and R_{40} and R_{90} subvolumes on PET_A. $A_{70} \cap R_{90}/R_{90}$ index was calculated at 0.69, meaning that two thirds of R_{40} was included in A_{70}. $A_{70} \cap R_{90}/R_{90}$ index was calculated at 1.00, meaning that R_{90} was totally included in A_{70}.

index were obtained with the same thresholds on PET_A. The 70% baseline SUV_{max} threshold showed moderate agreement (overlap fractions and $A_x \cap R_{90}/R_{90} > 0.51$) when compared with PET_B, PET_C, and PET_R. The Dice, Jaccard, and $A_x \cap R_{90}/A_x$ indices were very low (mostly <0.10) irrespective of the thresholds used on PET_A. The low variations between panels B, D, and F indicate that the position of the subvolumes was similar during the therapeutic sequence.

DISCUSSION

NSCLC is known to have high and heterogeneous ^{18}F-FDG uptake. A selective increase in radiotherapy dose to the most radioresistant areas within the tumor is tempting, as a way to improve local control rates without excessive toxicity. Along with others (*8–11*), we have shown in 39 patients (17 relapses) included in 3 prospective trials that intratumor subvolumes with high ^{18}F-FDG uptake (SUV > 70% SUV_{max}) can easily be delineated on staging PET scans to indicate areas at increased risk of relapse. This is of interest because the RTOG 0617 randomized trial (*20*) reported no benefit from an increased radiotherapy dose targeted on initial tumor volume on PET scans (SUV > 40% SUV_{max}). An alternative approach could be to delineate smaller target volumes, based on ^{18}F-FDG uptake (e.g., >70% SUV_{max}), that could receive total doses much higher than the conventional range (60–74 Gy). Very high precision in radiotherapy delivery is therefore required to avoid excessive irradiation of the normal tissues surrounding the target volume (*6,7, 21*). In addition, doses larger than 2 Gy per fraction can be delivered to shorten the overall radiotherapy duration, counterbalancing tumor cell proliferation and increasing the probability of cure. A prospective feasibility study of stereotaxic body radiotherapy after conventional therapy, increasing the total dose to residual disease above 100 Gy, showed no increase in acute toxicity compared with what was expected after conventional chemoradiotherapy (*21*).

Table 3 is a comparison with previous works. Abramyuk et al. (*8*) reported that the relapse volume defined with an automatic delineation method (ROVER; ABX Advanced Biochemical Compounds) was visually included in the initial volume defined with a 35% SUV_{max} threshold. Aerts et al. (*9,10*) compared retrospectively and prospectively the overlap fractions of initial subvolumes defined with 34%, 40%, 50%, 60%, 70%, and 80% SUV_{max} with relapse volumes defined with a fixed SUV threshold higher than 2.5% and 5%, aorta SUV, and relative threshold at 70%, 80%, and 90% SUV_{max}. Aerts proposed the 50% SUV_{max} threshold on initial PET scans as more suitable for the radiation-boosting target. More recently, Shusharina et al. (*11*), using a nonrigid coregistration method, prospectively compared the overlap fractions of an initial subvolume defined with the 50% SUV_{max} and a relapse subvolume defined with the 80% SUV_{max} threshold and confirmed Aerts' results.

After Aerts' first study (*22*) comparing overlap fractions of subvolumes defined with 34%, 40%, 50%, 60%, 70%, and 80% SUV_{max} at baseline (PET_A), at the seventh day of radiotherapy (PET_B), and at the 14th day of radiotherapy (PET_C), our results confirmed that the topography of the high ^{18}F-FDG uptake subvolumes within the tumor remains stable during the course of radiotherapy, despite large variations in absolute volumes. On the basis of these results, we conclude that residual metabolically active and relapse areas within the tumor can be identified using initial ^{18}F-FDG PET/CT scans.

Our present work, by relying on 5 different overlap indices, constitutes an extensive investigation. The disappointing values of the Dice and Jaccard indices can be attributed to very different absolute volumes (a ratio of more than 10 between A_{70} and R_{90}): two volumes with a good superimposition but a large difference in size will yield low Dice and Jaccard indices. Given the low resolution of ^{18}F-FDG PET/CT images and the uncertainties in

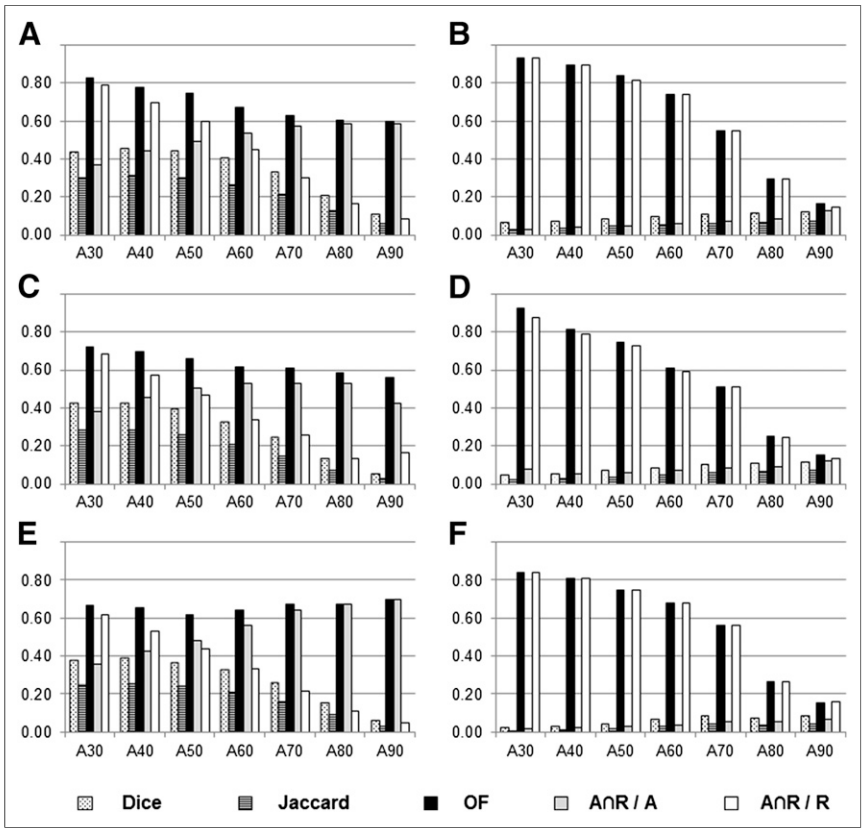

FIGURE 5. Histogram of mean values of overlap indices for various SUV_{max} thresholds (numeric indices refer to threshold for delineation) to delineate subvolumes on PET_A (A_X), PET_B (after induction chemotherapy, B_{40} and B_{90}, panels A and B), PET_C (C_{40} and C_{90}, panels C and D), and PET_R (R_{40} and R_{90}, panels E and F). Detailed data are presented in Supplemental Figure 1. OF = overlap fraction.

registration, A_{90} and R_{90} (same range of absolute volumes) were not likely to perfectly match.

We have investigated the ability of the $Ax \cap R_{40}/Ax$ and $Ax \cap R_{90}/R_{90}$ indices to better estimate the overlapping of potential target volumes for radiotherapy dose escalation with relapse volumes. We found that the baseline PET subvolume defined with the 70% SUV_{max} threshold is an acceptable choice for dose escalation to avoid missing the hot spot of recurrence (as shown by the $Ax \cap R_{90}/R_{90}$ index) and limit the irradiation of areas at a low risk of relapse (as shown by the $Ax \cap R_{40}/Ax$ index).

In our hands, these potential target volumes are 2–3 times smaller than those delineated by Aerts and Shusharina (mean, 12 cm^3; range, 0.6–51 cm^3; SD, 12 cm^3) and would allow higher dose escalation with stereotactic body radiotherapy. In agreement with others (*14,23*), the SUV_{max} at baseline or on planning ^{18}F-FDG PET was not significantly different in CR, DR, and LR patients.

In accordance with Aerts and our previous study (*9,14*), we have confirmed the association between persistent ^{18}F-FDG uptake during radiotherapy and poor outcome. The SUV_{max} on PET_C was significantly higher in locally relapsing patients than in patients with distant metastases or remission. We found that patients with an SUV_{max} of more than 5.6 or 5.9 during the fifth week of radiotherapy were at high risk of LR. As an attempt to reverse this poor prognosis, one could consider replanning stereotactic body radiotherapy with a higher total dose on PET/CT performed during the fifth week of radiotherapy, since most uptake and functional volume reduction has already occurred (*13*) and sufficient time is left to adapt the radiotherapy plan.

The present approach relies on careful coregistration of the sequential ^{18}F-FDG PET/CT images (117 coregistrations performed). We restricted our study to patients who were seen in a single institution, with images acquired under similar conditions and analyzed by two experienced physicians. Most of the difficulties occurred with follow-up ^{18}F-FDG PET/CT because of posttreatment alterations in morphology. Manual adjustment was allowed in cases of obvious misregistration until a consensus was obtained. The differences in overlap indices did not reach statistical significance between LR patients for whom coregistration did not need manual adjustment ($n = 7$) and LR patients who required manual adjustment ($n = 10$). This difference could be improved by using deformable registration techniques. However, these are difficult to validate and the reproducibility is limited. Respiratory gating was not required in our prospective trials. Strictly speaking, respiratory gating could have improved the precision of our results. Despite potential blurring due to respiratory movement, the clarity of our present results is nevertheless reassuring.

Our results apply to only the primary tumor site. Lymph node ^{18}F-FDG uptake was not investigated since local recurrence is usually at the site of the primary tumor. In addition, it would be difficult to increase the radiotherapy dose in 2 or more intrathoracic target volumes.

The subvolumes delineated on PET_A were followed on PET_B, PET_C, and PET_R subvolumes. We did not extensively investigate whether a similar approach could be applied to PET_B or PET_C. Our goal was to investigate the ability of a routine practice widely available—staging PET—to identify the intratumor site at high risk of relapse, whereas postchemotherapy preradiotherapy PET and per-radiotherapy PET are not accepted as part of clinical routine. As PET is increasingly used for radiotherapy planning, a recent prospective study showed that it is associated with higher overall survival rates in NSCLC patients (*24*); the ability of ^{18}F-FDG PET/CT performed after induction chemotherapy or during radiotherapy to identify the intratumor site at high of relapse has to be determined in future studies.

The small number of included patients is another limitation of our study. Our priority was to include carefully selected patients with complete clinical and imaging data available. Further confirmation requires prospective trials. Multivariate analysis was not performed since the population size was too small (lack of statistical power).

We did not use a specific tracer—such as ^{18}F-fluoromisonidazole—of hypoxia, a well-known factor of radioresistance. However, it has been reported that tumor hypoxia and ^{18}F-FDG uptake are related through the upregulation of glucose transporter 1 by

TABLE 3
Literature Review

Authors	Patients (*n*)	LR (*n*)	Time of ^{18}FDG PET/CT	Registration	Indices*	Defined and compared volumes†	Results
Aerts (▪)	17	—	A: d0 B: Per-RT d7 C: Per-RT d14	Rigid ± manual	OF	$A_{34–40–50–60–70–80}$ $B_{34–40–50–60–70–80}$ $C_{34–40–50–60–70–80}$	$OF_{34–60>0.70}$ $OF_{70–80>0.50}$
Abramyuk (*8*)	10	10	A: Pre-RT R: Post-RT m6–9	?	Visual	A_{35} R automatic (ROVER)	R visually included in A_{35} Threshold: 35% SUV_{max}
Aerts (▪)	55	22	A: Pre-RT R: Post-RT m3	Rigid ± manual	OF	$A_{34–40–50–60–70}$ $R_{70–80–90}$ $R_{>aorta}$; $R_{>2.5}$; $R_{>5}$	OF $A_{50}∩R_{>aorta}$ = 0.70 OF $A_{50}∩R_{80}$ = 077 OF $A_{50}∩R_{90}$ = 0.84 Threshold: 50% SUVmax
Aerts (▪)	12	7	A: Pre-RT R: Post-RT m3	Rigid ± manual	OF	$A_{34–40–50–60–70}$ $R_{70–80–90}$ $R_{>aorta}$	OF $A_{50}∩R_{>aorta}$ = 0.68 OF $A_{50}∩R_{90}$ = 0.74 Threshold: 50% SUVmax
Shusharina (*11*)	61	17	A: Pre-RT R: Post-RT d10 R: Post-RT m3 R: Post-RT m6	Nonrigid Derived Transformation Matrix	OF	A_{50} R_{80}	OF $A_{50}∩R_{d10}$ = 0.80 OF $A_{50}∩R_{m3}$ = 0.63 OF $A_{50}∩R_{m6}$ = 0.38 Threshold: 50% SUVmax
Present study	39	17	A: Pre-RT B: d0 C: Per-RT d21 R: Post-RT m3–12	Rigid ± manual	Dice Jaccard OF A∩R/A A∩R/R	$A_{30–40–50–60–70–80–90}$ B_{40} and $_{B90}$ C_{40} and $_{C90}$ R_{40} and $_{R90}$	$A_{70}∩R_{40}/A_{70}$ = OF $A_{70}∩R_{40}$ = 0.67 $A_{70}∩R_{90}/R_{90}$ = OF $A_{70}∩R_{90}$ = 0.56 $A_{60}∩R_{90}/R_{90}$ = OF $A_{60}∩R_{90}$ = 0.68 Threshold: 70% SUVmax

*Overlap quantification.
†Numeric indices refer to threshold for delineation.
d = days after radiotherapy began; m = months after radiotherapy began; OF = overlap fraction; RT = radiotherapy.
Threshold refers to recommended threshold for hot-spot delineation.

hypoxia-inducible factor 1 (*25,26*). ^{18}F-FDG and ^{18}F-fluoromisonidazole certainly give different but complementary information, and they can display similar intratumor distribution patterns (*27*). Although ^{18}F-FDG is not a specific hypoxia tracer, it is widely used and widely available, and its accumulation reflects overall metabolic activity and tumor load. Accordingly, targeting tumor subvolumes with an increased metabolic burden might be beneficial in tumor eradication (*28*).

CONCLUSION

Areas of high ^{18}F-FDG uptake on pretreatment PET/CT scans identify tumor subvolumes at greater risk of relapse in patients with NSCLC treated by concomitant chemoradiation. This result was obtained in 39 patients (17 relapses) included in a series of 3 prospective trials in a single institution. We provide further justification for clinical investigation of radiotherapy dose escalation in small target subvolumes delineated on initial ^{18}F-FDG PET/CT scans with a 70% SUV_{max} threshold.

DISCLOSURE

The costs of publication of this article were defrayed in part by the payment of page charges. Therefore, and solely to indicate this fact, this article is hereby marked "advertisement" in accordance with 18 USC section 1734. This study was supported by a grant from the Ligue Contre le Cancer de Haute Normandie and the North Ouest Canceropole (Institut National du Cancer; INCa). No other potential conflict of interest relevant to this article was reported.

ACKNOWLEDGMENT

We thank Sebastien Vauclin (DOSISoft) for his excellent collaboration.

REFERENCES

1. Goldstraw P, Ball D, Jett JR, et al. Non-small-cell lung cancer. *Lancet.* 2011;378: 1727–1740.
2. Albain KS, Swann RS, Rusch VW, et al. Radiotherapy plus chemotherapy with or without surgical resection for stage III non-small-cell lung cancer: a phase III randomised controlled trial. *Lancet.* 2009;374:379–386.
3. Garg S, Gielda BT, Kiel K, et al. Patterns of locoregional failure in stage III non-small cell lung cancer treated with definitive chemoradiation therapy. *Pract Radiat Oncol.* 2014;4:342–348.
4. Machtay M, Bae K, Movsas B, et al. Higher biologically effective dose of radiotherapy is associated with improved outcomes for locally advanced non-small cell lung carcinoma treated with chemoradiation: an analysis of the Radiation Therapy Oncology Group. *Int J Radiat Oncol Biol Phys.* 2012;82:425–434.
5. Machtay M, Paulus R, Moughan J, et al. Defining local-regional control and its importance in locally advanced non-small cell lung carcinoma. *J Thorac Oncol.* 2012;7:716–722.
6. Bayman N, Blackhall F, McCloskey P, Taylor P, Faivre-Finn C. How can we optimise concurrent chemoradiotherapy for inoperable stage III non-small cell lung cancer? *Lung Cancer.* 2014;83:117–125.
7. Timmerman RD, Herman J, Cho LC. Emergence of stereotactic body radiation therapy and its impact on current and future clinical practice. *J Clin Oncol.* 2014;32:2847–2854.
8. Abramyuk A, Tokalov S, Zöphel K, et al. Is pre-therapeutical FDG-PET/CT capable to detect high risk tumor subvolumes responsible for local failure in non-small cell lung cancer? *Radiother Oncol.* 2009;91:399–404.
9. Aerts HJWL, van Baardwijk AAW, Petit SF, et al. Identification of residual metabolic-active areas within individual NSCLC tumours using a pre-radiotherapy 18fluorodeoxyglucose-PET-CT scan. *Radiother Oncol.* 2009;91:386–392.
10. Aerts HJ, Bussink J, Oyen WJ, et al. Identification of residual metabolic-active areas within NSCLC tumours using a pre-radiotherapy FDG-PET-CT scan: a prospective validation. *Lung Cancer.* 2012;75:73–76.
11. Shusharina N, Cho J, Sharp GC, Choi NC. Correlation of ^{18}F-FDG avid volumes on pre–radiation therapy and post–radiation therapy FDG PET scans in recurrent lung cancer. *Int J Radiat Oncol Biol Phys.* 2014;89:137–144.
12. van Elmpt W, De Ruysscher D, van der Salm A, et al. The PET-boost randomised phase II dose-escalation trial in non-small cell lung cancer. *Radiother Oncol.* 2012;104:67–71.
13. Edet-Sanson A, Dubray B, Doyeux K, et al. Serial assessment of FDG-PET FDG uptake and functional volume during radiotherapy (RT) in patients with non-small cell lung cancer (NSCLC). *Radiother Oncol.* 2012;102:251–257.
14. Vera P, Mezzani-Saillard S, Edet-Sanson A, et al. FDG PET during radiochemotherapy is predictive of outcome at 1 year in non-small-cell lung cancer patients: a prospective multicentre study (RTEP2). *Eur J Nucl Med Mol Imaging.* 2014;41:1057–1065.
15. Thureau S, Chaumet-Riffaud P, Modzelewski R, et al. Interobserver agreement of qualitative analysis and tumor delineation of ^{18}F-fluoromisonidazole and 3′-deoxy-3′-^{18}F-fluorothymidine PET images in lung cancer. *J Nucl Med.* 2013;54:1543–1550.
16. Paidpally V, Mercier G, Shah BA, Senthamizhchelvan S, Subramaniam RM. interreader agreement and variability of FDG PET volumetric parameters in human solid tumors. *AJR.* 2014;202:406–412.
17. Erdi YE, Mawlawi O, Larson SM, et al. Segmentation of lung lesion volume by adaptive positron emission tomography image thresholding. *Cancer.* 1997;80(12, suppl):2505–2509.
18. Ourselin S, Roche A, Prima S, Ayache N. Block matching: a general framework to improve robustness of rigid registration of medical images. In: *Medical Image Computing and Computer-Assisted Intervention–MICCAI 2000.* New York, NY: Springer; 2000:557–566.
19. Hanna GG, Hounsell AR, O'Sullivan JM. Geometrical analysis of radiotherapy target volume delineation: a systematic review of reported comparison methods. *Clin Oncol (R Coll Radiol).* 2010;22:515–525.
20. Bradley JD, Paulus R, Komaki R, et al. A randomized phase III comparison of standard-dose (60 Gy) versus high-dose (74 Gy) conformal chemoradiotherapy with or without cetuximab for stage III non-small cell lung cancer: results on radiation dose in RTOG 0617 [abstract]. *J Clin Oncol.* 2013;31(suppl):7501.
21. Feddock J, Arnold SM, Shelton BJ, et al. Stereotactic body radiation therapy can be used safely to boost residual disease in locally advanced non-small cell lung cancer: a prospective study. *Int J Radiat Oncol Biol Phys.* 2013;85:1325–1331.
22. Aerts HJ, Bosmans G, van Baardwijk AA, et al. Stability of ^{18}F-deoxyglucose uptake locations within tumor during radiotherapy for NSCLC: a prospective study. *Int J Radiat Oncol Biol Phys.* 2008;71:1402–1407.
23. Lin M-Y, Wu M, Brennan S, et al. Absence of a relationship between tumor ^{18}F-fluorodeoxyglucose standardized uptake value and survival in patients treated with definitive radiotherapy for non–small-cell lung cancer. *J Thorac Oncol.* 2014;9:377–382.
24. Mac Manus MP, Everitt S, Bayne M, et al. The use of fused PET/CT images for patient selection and radical radiotherapy target volume definition in patients with non-small cell lung cancer: results of a prospective study with mature survival data. *Radiother Oncol.* 2013;106:292–298.
25. Mees G, Dierckx R, Vangestel C, Laukens D, Van Damme N, Van de Wiele C. Pharmacologic activation of tumor hypoxia: a means to increase tumor 2-deoxy-2-[^{18}F]fluoro-D-glucose uptake? *Mol Imaging.* 2013;12:49–58.
26. van Baardwijk A, Dooms C, van Suylen RJ, et al. The maximum uptake of ^{18}F-deoxyglucose on positron emission tomography scan correlates with survival, hypoxia inducible factor-1α and GLUT-1 in non-small cell lung cancer. *Eur J Cancer.* 2007;43:1392–1398.
27. Huang T, Civelek AC, Li J, et al. Tumor microenvironment-dependent ^{18}F-FDG, ^{18}F-fluorothymidine, and ^{18}F-misonidazole uptake: a pilot study in mouse models of human non-small cell lung cancer. *J Nucl Med.* 2012;53:1262–1268.
28. Wijsman R, Kaanders JH, Oyen WJ, Bussink J. Hypoxia and tumor metabolism in radiation oncology: targets visualized by positron emission tomography. *Q J Nucl Med Mol Imaging.* 2013;57:244–256.